Fluorescence Quenching and Binding Interaction of 10-Methylacridinium Iodide to Nucleic Acids

SUN, Xian-Feng(孙险峰) JIANG, Zhi-Qin*(江致勤) DING, Bing-Lin(丁兵林)
Department of Chemistry, Tongji University, Shanghai 200092, China

Interaction of 10-methylacridinium iodide (MAI) as fluorescence probe with nucleobases, nucleosides and nucleic acids has been studied by UV-visible absorption and fluorescence spectroscopy. It was found that fluorescence of MAI is strongly quenched by the nucleobases, nucleosides and nucleic acids, respectively. The quenching follows the Stern-Volmer linear equation. The fluorescence quenching rate constant (k_q) was measured to be 10^9—10^{10} (L/mol)/s within the range of diffusion-controlled rate limit, indicating that the interaction between MAI and nucleic acid and their precursors is characteristic of electron transfer mechanism. In addition, the binding interaction model of MAI to calf thymus DNA (ct-DNA) was further investigated. Apparent hypochromism in the absorption spectra of MAI was observed when MAI binds to ct-DNA. Three spectroscopic methods, which include (1) UV spectroscopy, (2) fluorescence quenching of MAI, (3) competitive dual-probe method of MAI and ethidium bromide (EB), were utilized to determine the affinity binding constants (K) of MAI and ct-DNA. The binding constants K obtained from the above methods gave consistent data in the same range (1.0—5.5) × 10^4 L/mol, which lend credibility to these measurements. The binding site number was determined to be 1.9. The influence of thermal denaturation and phosphate concentration on the binding was examined. The binding model of MAI to ct-DNA including intercalation and outside binding was investigated.

Keywords DNA, fluorescence probe, quenching, binding interaction, denaturation

Introduction

In recent years, luminescent probe, particularly, fluorescence probe of nucleic acid (NA) and its precursor (NP) including nucleobase, nucleoside and nucleotide has become one of the most powerful tools in the study of NA. It is well known that there is versatile interaction between nucleic acid and exogenous substrates such as hydrogen bond, electrostatic action, stacking and van der Waals force *etc*.,[1] which basically belongs to the physical interaction. However, the latest progress in this area has shown that electron transfer (ET) process of nucleic acid with endogenous and exogenous substrates initially induces hole transport along the nuclear acid chain. These chemical interactions eventually cause significant mutation of base side-chain or cleavage of nucleic acid strand.[2-5] Besides, there have been intensive studies on elucidating factors that determine affinity and selectivity in binding of small molecules to DNA.[6] Quantitative understanding of such factors that affect recognition site and ability of DNA should be valuable in the rational design of sequence-specific DNA binding molecules for application in chemotherapy and in the development of tools for biotechnology. It is very important in bioorganic chemistry to know that how the molecular structure and the biological function of a nucleic acid are influenced by small molecules such as probe under different conditions. The interaction of acridine dyes with DNA is of special interest because of their unique binding activity.[7] Optical methods, particularly fluorescence methods, are the most useful methods for the study of the binding interaction because of the high sensitivity to the environment.

In this paper, a cationic heterocyclic dye, 10-methyl acridinium iodide (MAI) (Fig. 1), was employed as a probe for the study of its interaction with nucleic acids and their precursors. With UV-visible absorption and fluorescence spectroscopic methods, the Stern-Volmer quenching and Scatchard correlation were further utilized to measure the quenching rate constant, the apparent binding constant and the binding site number in base pairs. These results reveal the electron transfer quenching mechanism of fluorescence probe MAI and intercalation binding modes with DNA and RNA.

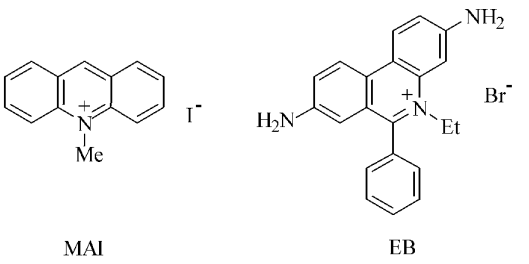

MAI EB

Fig. 1 Structures of compounds MAI and EB.

* E-mail: zqjiang@mail.tongji.edu.cn
Received May 22, 2002; revised and accepted July 2, 2003.
Project supported by the National Natural Science Foundation of China (Nos. 20072028 and 20272042).

Experimental

Chemicals

10-Methyl acridinium iodide (MAI) was prepared according to the reported method,[8] recrystallized from alcohol/water, m.p. 249—250 ℃. Ethidium bromide (EB), calf thymus DNA (ct-DNA), salmon sperm DNA (ss-DNA), yeast RNA (y-RNA) and sodium dodecyl sulfate (SDS) were purchased from Sino-American Biotechnological Co. (Shanghai) and used without further purification. Adenine (ADN) and hypoxanthine (HXT) were Fluka reagents. Uracil (URA), uridine (URD), thymine (THM) and cytosine (CTS) were commercial available from Sino-American Biotechnological Co. (Shanghai). Guanosine (GS), deoxyguanosine (DGS) and deoxyuridine (DURD) were Aldrich reagents. These nitrogeneous bases and nucleosides were recrystallized respectively from twice distilled water. All samples were dissolved in 5 mmol/L of Tris-HCl buffer at pH = 7.2 and 50 mmol/L of NaCl solution unless mentioned otherwise.

Instruments and methods

All the UV-visible absorption spectra were recorded on a Lambda Bio-40 UV-vis spectrophotometer. Fluorescence spectra were recorded on a Perkin Elmer LS-50 fluorophotometer. Fluorescence lifetime was measured on a Horiba NAES-1100 single photo-counting transient spectrometer with a multi-channel analyzer.

The concentration of nucleic acid in buffer solution was determined by UV absorbance at 260 nm by using ε (DNA) = 6600 cm^2/mol.[9] The absorbance ratio of NA was determined as $A_{260}/A_{280} = 1.8—1.9$, indicating the purity of NA used was eligible.

Denaturation of DNA was carried out by boiling in water for 30 min in tightly capped vials and by cooling in ice-water, stored frozen before use. When needed for experiments, it was thawed and boiled for 5 min, and cooled to room temperature in ice-water. In experiments the higher concentration of sodium chloride was used (> 20 mmol/L), and the salt was added just prior to measurement in order to minimize renaturation.

For intercalation studies the temperature was maintained at 25 ℃. The intrinsic binding constant (K) of MAI with DNA was determined by absorption and fluorescence titration. The titration was performed by varying the nucleic acid concentration and by keeping the concentration of the probe constant. In the former case, the absorbance at 357.5 nm was recorded with increasing the concentration of DNA, whereas fluorescence intensity of MAI was monitored at 486 nm.

Results and discussion

Fluorescence quenching of MAI

Cationic dye MAI as fluorescence probe (excitation energy, $E_{0,0}$ = 2.77 eV)[8] possesses strong electron-accepting ability ($E_{red} = -0.37$ V vs. SCE),[9] whereas the oxidation potentials (E_{ox}) of NA and its precursor NP were known in the range of 1.1—1.8 V.[2,9] Therefore, the driving force for the primary photoinduced electron transfer (PTE) process [Eq. (1)] from the ground states of NA and NP to the singlet state of MAI can be predicted from the Rehm-Weller equation.[10]

$$(MA^+)^1 + NA \text{ (or NP) } MA. + NA^{+\cdot} (OR\ NP^{+\cdot}) \quad (1)$$

Calculation from the above data and equation gave the free energy change ΔG from − 57.7 kJ/mol to − 115.8 kJ/mol. The negative values of ΔG clearly imply that these primary PET processes are thermodynamically favored.

Fluorescence quenching technique is an important method to study the electron transfer and energy transfer processes.[11] The fluorescence quenching of MAI by a series of NP and NA as quenchers was measured. The quenching was found to follow the static and dynamic Stern-Volmer linear correlation [Eqs. (2), (3)]:[11]

$$I_0/I = 1 + k_q(s)\tau_0 \quad [Q] \quad (2)$$

$$\tau_0/\tau = 1 + k_q(d)\tau_0 \quad [Q] \quad (3)$$

Herein I_0 and I are the fluorescence intensities of a probe in the absence and presence of quencher Q, respectively. τ_0 and τ are the fluorescence lifetimes in the absence and presence of the quencher Q, respectively. Fig. 2 shows both the static and dynamic Stern-Volmer linear plots of I_0/I and τ_0/τ vs. [THM]. The τ_0 value of MAI was measured to be 9.50 and 9.87 ns in SDS and H_2O, respectively. The static and dynamic quenching rates, $k_q(s)$ and $k_q(d)$, were determined from the plot slopes and τ_0.

All the quenching data for a series of nucleobases, DNA and RNA are listed in Tables 1 and 2. The data indi-

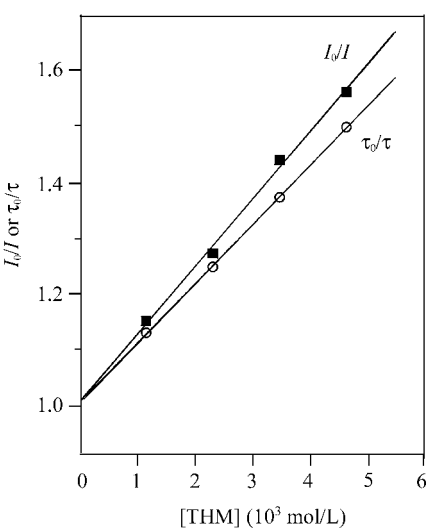

Fig. 2 Static and transient Stern-Volmer plots of fluorescence quenching of MAI by THM in SDS. [MAI] = 5.73×10^{-5} mol/L; [SDS] = 2.0×10^{-2} mol/L; λ_{ex} = 400 nm, λ_{em} = 490 nm.

cate that the fluorescence of MAI is significantly quenched by these NP and NA quenchers and values of k_q(s) and k_q(d) are in the order of 10^{10} L·mol^{-1}·s^{-1}, near the diffusion-controlled limit rate. This implies that the quenching is characteristic of the singly electron transfer (SET) mechanism as illustrated by Eq. (1), which coincides with the reported ET mechanism for the interaction of a series of electron-deficient dyes to DNA using varies spectral and electro-chemical means. In addition, the quenching of MAI by DNA or RNA such as ct-DNA, ss-DNA and y-RNA were found to be stronger than that by nucleic acid precursors *e.g.* nucleobases and nucleosides.

Table 1 Fluorescence quenching data of MAI by nucleobases[a]

Quencher	k_q(s) (L·mol^{-1}·s^{-1})	k_q(d) (L·mol^{-1}·s^{-1})
URA	5.85	—
ADE	9.50	6.65
HXZ	3.29	—
THY	3.32	2.92
CYT	3.74	—

[a] k_q(s) $\times 10^{-9}$, k_q(d) $\times 10^{-9}$.

Table 2 Fluorescence quenching data of MAI by nucleobases and NA[a]

Quencher	k_q(s)[a] (L·mol^{-1}·s^{-1})	r
URD	0.83	0.998
DURD	5.48	0.998
GS	7.26	0.999
DGS	7.29	0.997
ct-DNA	34.5	0.999
ss-DNA	15.6	0.997
y-RNA	26.5	0.998

[a] k_q(s) $\times 10^{-9}$.

The quenching ability shows the following sequence: DNA ~ RNA > NP (nucleobase, nucleoside). This general behavior of ET-type of quenching interaction of electron-deficient MA$^+$ by NA and NP can be interpreted as follows.

The electron-donating power of NP is due to its unshared electron pair at ntrogen atom and the multi-nitrogen in the base pair region of NA should make NA to have even stronger electron-donating ability.

Binding of probe MAI *to* DNA

In order to study further the binding interaction model and mechanism of MAI to DNA, three spectroscopic methods were utilized to determine the apparent affinity binding constants of MAI with ct-DNA. They include (1) UV spectroscopic measurement, (2) fluorescence quenching of MAI and (3) the competitive fluorescence method of dual probe, MAI and EB. The results can reveal the binding ability, binding site number and model as well.

UV *spectroscopic determination* Fig. 3a shows the UV-visible spectra of MAI with increasing ct-DNA concentration. The absorption band of MAI at 360 nm decreases rapidly with the increase in ct-DNA concentration and isobestic points at 365 and 338 nm were observed. This pronounced hypochromism at 360 nm indicates a close proximity of MAI to the ct-DNA base pairs, and probably it is a result of strong intercalation of the MAI probe into the base pairs of ct-DNA. Moreover, the wide absorption bands longer than 365 nm may imply the complex formation of MAI-DNA in the ground states. To verify this complex formation, the absorption titration experiment was performed according to the Eq. (4).[12,13]

$$1/\varepsilon_a - \varepsilon_F = 1/c(\varepsilon_B - \varepsilon_F)K + 1/\varepsilon_B - \varepsilon_F \quad (4)$$

A reciprocal plot of $1/\varepsilon_a - \varepsilon_F$ vs. $1c$ gave a linear correlation (Fig. 3b), where c = [ct-DNA] and the apparent extinction coefficient ε_a was obtained by calculating A/[MAI]. ε_B and ε_F correspond to the extinction coefficient of the bound form of MAI and the titration coefficient of the free form of MAI, respectively. With the ratio of the slop and intercept from Eq. (4) the apparent affinity binding

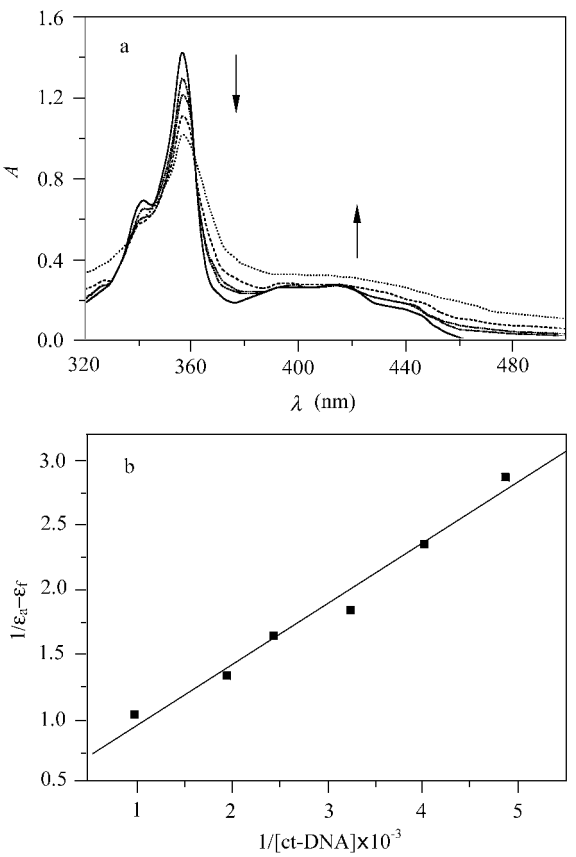

Fig. 3 (a) Absorption spectra of MAI with increase of [ct-DNA]; (b) Reciprocal plot of $1/\varepsilon_a - \varepsilon_F$ vs. 1/[ct-DNA], [MAI] = 6.25×10^{-5} mol/L; [ct-DNA] = 0, 2×10^{-4}, 2.5×10^{-4}, 3×10^{-4}, 4×10^{-4}, 5×10^{-4} and 10×10^{-4} mol/L from top to bottom.

constant was determined as $K = 1.4 \times 10^4$ L/mol in base pairs.

It is demonstrated that when the double helix of ct-DNA was denatured, the absorption spectrum of MAI restored to the same shape and intensity of the free probe. This result verifies that the UV hypochromism of MAI at 360 nm and wide band of the complex above 365 nm in the presence of ct-DNA was due to the intercalation of MAI into the double helix of DNA.

Fluorescence quenching of MAI Binding of the probe MAI to the DNA helix was found to quench the probe fluorescence very strongly. Thus, the fluorescence intensity of MAI decreases rapidly with increasing concentration of ct-DNA (Fig. 4). The fluorescence quenching constant $[(K_{SV} = k_q(s)\tau_0)]$ evaluated from the Stern-Volmer Eq. (2) and the plot slop was 1×10^3 L/mol of ct-DNA (see Fig. 2). With the fluorescence lifetime of MAI, $\tau_0 = 32.5$ ns, it gave the quenching rate constant k_q of 3.5×10^{10} L·mol^{-1}·s^{-1}.

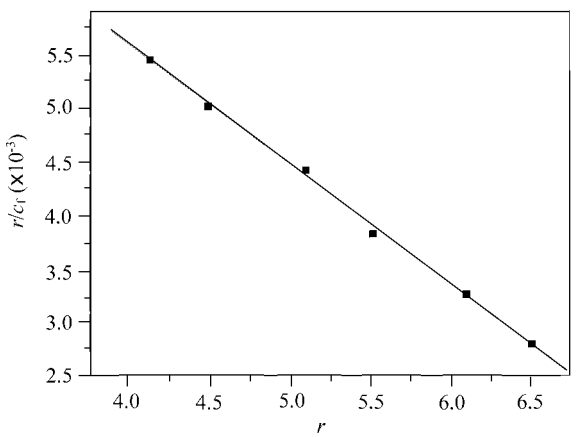

Fig. 4 Scatchard plot of r/c_f vs. r for binding of MAI to ct-DNA by fluorescence quenching. [MAI] = 6.25×10^{-5} mol/L; [ct-DNA] = 0, 2×10^{-4}, 3×10^{-4}, 4×10^{-4}, 5×10^{-4} and 10×10^{-4} mol/L from top to bottom; $\lambda_{ex} = 380$ nm, $\lambda_{em} = 480$ nm.

According to the modified Scatchard Eq. (5) proposed by McGhee and von Hippel,[14] where K_i is the apparent binding constant and n the binding site number in base pairs, the concentration of the probe can be calculated by Eq. (6).

$$r/c_f = K_i(1 - nr)\{(1 - nr)/[1 - (n - 1)r]\}^{n-1} \quad (5)$$

$$c_F = c_T(I/I_0 - P)/(1 - P) \quad (6)$$

Herein c_T and c_F are the total concentration of the probe added and the concentration of the free probe, respectively. P is the ratio of the observed fluorescence intensity of the bound probe to that of the free probe. The value of P was determined from the intercept in the plot of I/I_0 versus 1/[DNA]. The concentration of the bound probe (c_B) equals ($c_F - c_T$). Thus, the Scatchard plot of r/c_f vs. r gives rise to the apparent binding constant $K_i = 1.03 \times 10^4$ L/mol, $n = 1.9$ in base pairs.

Competitive fluorescence method of MAI *and* EB

Apparent binding constant was also measured by competition of MAI with EB. EB is known as an important stain reagent for DNA. The advantage of this competition assay is that the fluorescence of EB in the absence of DNA is very weak, however, fluorescence of EB increases apparently when EB intercalates into ct-DNA. In contrast, the fluorescence of MAI decreases rapidly as MAI intercalates into ct-DNA. Based on this opposite fluorescence behavior of the dual-probe complex, MAI- DNA-EB, a competitive fluorescence quenching method of the dual-probe is developed to determine the binding constant. Thus, the measurement of the fluorescence intensity of EB bound to DNA was carried out in the presence of various concentrations of the second probe, MAI. Considering the second probe competitor, the Scatchard analysis was modified as shown in Eq. (7),[13] where K is the intrinsic binding constant of EB to DNA in the absence of MAI. K' represents the binding constant of the competitor (MAI) and K_{obs} is the binding constant of EB in the presence of the competitor. c_f' is the concentration of free competitor such as MAI.

$$1/K_{obs} = (K'/K)c_f' + 1/K \quad (7)$$

The decrease of fluorescence of EB-ct-DNA complex with various concentrations of the competitor MAI allows the determination of the apparent binding constant K' of MAI to ct-DNA according to Le Pecq and Paoletti.[15] Fig. 5 shows three Scatchard linear plots (a—c) for the binding of EB to ct-DNA with different concentration of MAI (from 0 to 1.25 μmol/L) according to the Eq. (5), which gives three values of K_{obs}. Then, the binding constant of MAI to

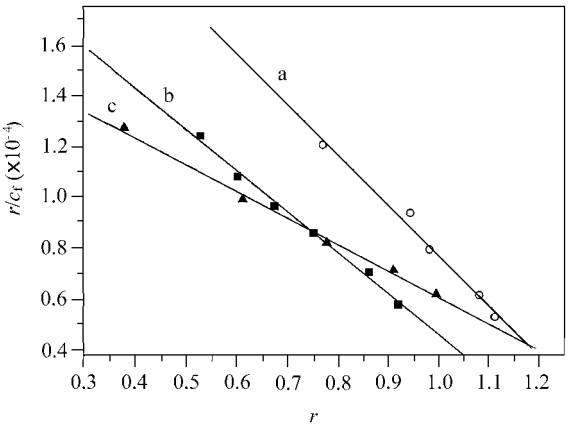

Fig. 5 Scatchard plots for the binding of EB to ct-DNA with competition of MAI. (a) [MAI] = 0 μmol/L, $K_{obs} = 1.92 \times 10^5$ L/mol; (b) [MAI] = 0.60 μmol/L, $K_{obs} = 1.31 \times 10^5$ L/mol; (c) [MAI] = 1.25 μmol/L, $K_{obs} = 1.11 \times 10^5$ L/mol; [EB] = 2.5×10^{-5} mol/L; $\lambda_{ex} = 525$ nm, $\lambda_{em} = 590$ nm.

ct-DNA was obtained as $K' = 5.53 \times 10^4$ L/mol from the linear plot of $1/K_{obs}$ vs. [MAI] by the Eq. (7).

In summary, the above three spectroscopic methods give consistent binding constants of MAI in the range (1×10^4—5.5×10^4 L/mol) which lend credibility to these measurements. In addition, the high affinity and strong interaction of MAI to ct-DNA indicated by K value is closely related to the binding model as discussed later.

Other influence factors on the binding

Effect of phosphate concentration

In the buffer medium, MAI and NaH_2PO_4 was added into DNA-EB solution. With the increase of phosphate concentration, the relative fluorescence intensity of MAI-DNA-EB system increases drastically, as shown in Table 3. The experimental results demonstrate that phosphate ions weakened the interaction of the MAI and DNA because phosphate anion of NaH_2PO_4 competes with the phosphate group of the ct-DNA in binding to cation MA^+, and thus weakens the fluorescence quenching of MAI-DNA-EB ligand. Hence, it could be concluded that the MAI can interact with the ct-DNA phosphate backbone by electrostatic binding.

Table 3 Effect of phosphate ions on the fluorescence intensity of MAI-DNA-EB complex[a]

[NaH_2PO_4] (10^{-4} mol/L)	0	2.5	5.0	10.0	25.0	50.0
Relative fluorescence intensity (%)	10.05	13.17	16.58	25.96	40.21	56.34

[a] [DNA] = 2.52×10^{-4} mol/L, [EB] = 1.24×10^{-5} mol/L, [MAI] = 5.00×10^{-5} mol/L.

Effect of ds-DNA *and* ss-DNA *on the fluorescence quenching of* MAI

The single strand ct-DNA (ss-ct-DNA) was obtained by thermal denaturation of the double strand DNA (ds-ct-DNA). The effects of ds-ct-DNA and ss-ct-DNA on the fluorescence quenching of MAI were performed. The Stern-Volmer plots were shown in Fig. 6. It was found that the fluorescence quenching of the dye MAI by ds-ct-DNA is about 1.8 stronger fold than that by ss-ct-DNA in terms of the fluorescence quenching rate constants k_q. This implies that the dye MAI intercalates into the helix stack of ds-ct-DNA very strong because the helix stacks of ds-ct-DNA were destroyed to ss-ct-DNA during the denaturation. Otherwise, if the dye had bound to DNA in a non-intercalation mode, the denaturation of DNA would have had little effect on the fluorescence quenching of the dye. Accordingly, this phenomenon further confirmed that MAI intercalates into the helix stack of ds-ct-DNA.

The influence of the melting point T_m on the binding of MAI to ct-DNA was also measured. It was observed that T_m of ct-DNA was 78 ℃ in the absenceof the probe MAI (Fig. 7b), whereas raised to 84 ℃ when MAI was present (Fig. 7a). This phenomenon illustrates that the intercalative binding of MAI to ct-DNA will enhance the stability of the double strand ct-DNA, being consistent with the case of the intercalation of EB to DNA.

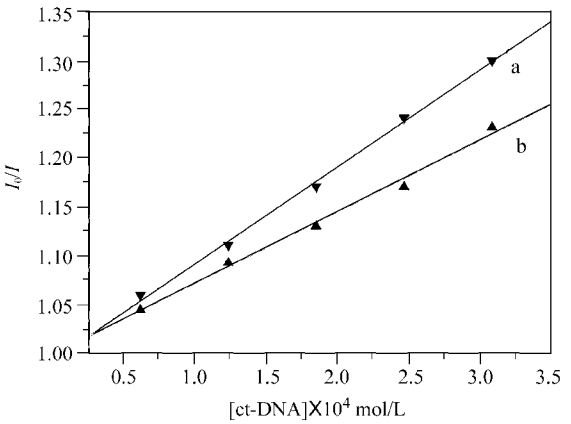

Fig. 6 Stern-Volmer plots for MAI/ct-DNA system. (a) ds-ct-DNA, $k_q = 3.5 \times 10^{10}$ (L/mol)/s; (b) ss-ct-DNA, $k_q = 2.0 \times 10^{10}$ (L/mol)/s.

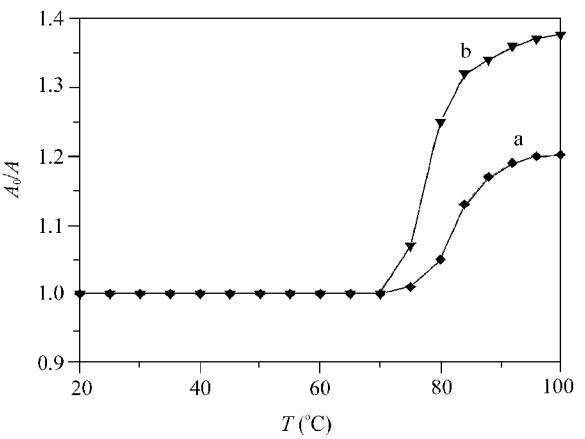

Fig. 7 Thermal denaturation of ct-DNA and plot of A_0/A vs. T. (a) [MAI] = 6.25×10^{-5}mol/L; (b) [MAI] = 0 mol/L; [ct-DNA] = 2.5×10^{-4} mol/L; λ_{obs} = 260 nm.

Binding model of MAI *to* DNA

The binding of a small molecular probe to DNA has been intensively investigated.[16-20] In general, there are two types of binding ways: territorial binding and site binding. In territorial binding, the ligands interact with the DNA phosphate groups by the electrostatic Coulomb force but they are not associated with any specific site or group of sites, *i.e.*, they move free around the DNA skeleton. Therefore, this outside binding is comparably weak. In site binding, the ligands associate with one or more specific sites on the DNA. In particular, if the ligand is a cationic dye (electron-deficient), the fused aromatic cation of the dye tends to intercalate between the adjacent

base-pair planes of DNA because the multi-nitrogen region of the adjacent base-pair planes is of electron-rich, hence this intercalation is much stronger than the former binding. The two binding models are depicted below in Fig. 8. In the preceding experiments, it is demonstrated that the fluorescence of MAI is strongly quenched by NP and NA via the ET mechanism. The electron-deficient MAI is a fused tricycle-cation, which can insert, vertical to the axis of DNA helix and in sandwich-like, into the adjacent layers consisting of electron-rich base pairs. This strong binding of MAI to ct-DNA may enhance the ETs interaction and is proved by the measurement of large K values. The thermal denaturation of ct-DNA also indicates that the intercalation binding the model is major one in this work. Finally, the anionic influence of $H_2PO_4^{-1}$ on the binding of MAI to ct-DNA implies that the outside binding should be a minor model. Therefore, the binding mode is dependent on the structure of small molecule and DNA, as well as the ionic strength of the medium.

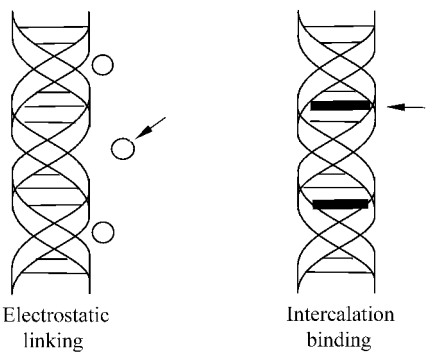

Fig. 8 Binding model of probe (O) to DNA.

Conclusion

The fluorescence of MAI was quenched by NP and NA strongly. The quenching follows very well the Sterm-Volmer linear equation. The quenching rate constants k_q lie in the region of the diffusion-controlled limit [*ca*. 10^{10} $L \cdot mol^{-1} \cdot s^{-1}$], which is an indication of the electron transfer interaction between MAI and NA. On binding study of MAI to DNA, the strong binding constants in the order of 10^4 L/mol measured by three optical methods verify that MAI binds to the double helix of ct-DNA in a interaction binding model. The experiments in thermal denaturation and anionic effect further support the intercalation mechanism of the dye to ct-DNA.

References

1 Wang, Y. C.; Yuan, Y. F.; Ding, B. L.; Wang, P. J.; Sun, X. F.; Dai, B.; Wu, S. P.; Jiang, Z. Q. *Chin. J. Org. Chem.* **2001**, *21*, 893 (in Chinese).
2 Ly, D.; Sanii, L.; Schuster, G. B. *J. Am. Chem. Soc.* **1999**, *121*, 9400.
3 Armitage, B. *Chem. Rev.* **1998**, *98*, 1171.
4 Burrows, C. J.; Muller, J. G. *Chem. Rev.* **1998**, *98*, 1109.
5 Prat, F.; Houk, K. N.; Foote, C. S. *J. Am. Chem. Soc.* **1998**, *120*, 845.
6 Bixon, M.; Jortner, J. *Electron Transfer From Isolated Molecules to Biomolecules*, John Wiley & Sons, New York, **1999**.
7 Steiner, R. F. *Excited States of Biopolymer*, Plenium Press, New York, **1983**, pp. 163—250.
8 Kavarnos, G. J.; Turro, N. *J. Chem. Revs.* **1986**, *86*, 401.
9 Wu, S. P.; Ding, B. L.; Wu, J. B.; Jiang, Z. Q. *Res. Chem. Intermed.* **2000**, *26*, 727.
10 Rehm, D.; Weller, A. *Isr. J. Chem.* **1970**, *8*, 259.
11 Lakowicz, J. R. *Principles of Fluorescence Spectroscopy*, Plenum Press, New York, **1983**.
12 Pyle, A. M.; Rehmann, J. P.; Meshoyrer, R.; Kumar, C. V. *J. Am. Chem. Soc.* **1989**, *111*, 3051
13 Dougherty, G.; Pilbrow, J. R. *Int. J. Biochem.* **1985**, *24*, 1179.
14 (a) McGhee, J. D.; Von Hipple, P. H. *J. Mol. Biol.* **1974**, *86*, 469.
(b) Lepecq, J. B.; Paoletti, C. J. *J. Mol. Biol.* **1967**, *27*, 87.
15 Barton, J. K. *Science* **1986**, *233*, 727.
16 Wade, W. S.; Dervan, P. B. *J. Am. Chem. Soc.* **1987**, *109*, 1574.
17 Caceres-Cortes, J.; Sugiyama, H.; Ikudome, K.; Saito, I.; Wang, A. H. *J. Biochem.* **1997**, *36*, 9995.
18 Neault, J. F.; Tajmir-Riahi, H. A. *J. Phys. Chem., B* **1998**, *102*, 1610.
19 Mahadevan, S.; Palaniandavar, M. *Inorg. Chem.* **1998**, *37*, 3927.

(E0205221 SONG, J. P.)